

# GRAVITY AND MAGNETIC FIELDS OF POLYGONAL PRISMS AND APPLICATION TO MAGNETIC TERRAIN CORRECTIONS

DONALD PLOUFF\*

Computer programs based on the exact calculations of the gravity and magnetic anomalies of polygonal prisms are faster in operation and more accurate than previous programs based on the numerical integration of polygonal laminas. The prism programs also are of more general application than existing computer programs that are based on the exact gravity and magnetic effects of rectangular prisms. There are no restrictions on the use of the exact formula for the gravitational attraction of a polygonal prism, but the formulas for the magnetic effect are restricted in that demagnetization is not considered, and a finite answer is not obtained in the unrealistic circumstance where an observation point coincides with an edge of the prism.

Least-squares methods permit calculation of the gravity or magnetic effect of models without

knowledge of the density or magnetization contrasts, respectively, by comparison of the observed anomalies with theoretical dimensionless values to determine contrasts as regression coefficients. The coefficient of correlation provides a goodness of fit estimate that helps model evaluation. After calculating a magnetic terrain correction for an outcrop of Quaternary dacite and andesite near Clear Lake, Calif., an improvement of the coefficient of correlation from 88 to the 92 percent level indicates that this volcanic unit probably extends at least 150 m beneath the surface. Application of a magnetic terrain correction to disconnected outcrops of Tertiary andesite, eliminates most of a prominent v-shaped magnetic anomaly south of the San Juan Mountains, Colo.

## INTRODUCTION

Talwani and Ewing (1960) suggested a method to calculate the gravity anomaly of a three-dimensional body by numerical integration of horizontal polygonal laminas that approximate the shape of the body. Bott (1963) and Talwani (1965) later suggested methods to calculate components of the magnetic field of a horizontal lamina with a polygonal boundary. Computer programs that implement the methods have proved valuable in three-dimensional gravity and magnetic interpretation.

A three-dimensional body can be represented by summing a number of horizontal laminas that compose the entire body. A lamina replaces a polygonalized contour from the total body. The

greater the height of observation compared to the thickness represented by each lamina, the more accurate will be the result of the numerical integration. The use of Simpson's rule in Talwani's computer programs minimizes the error resulting from numerical integration and permits bodies to be terminated at the top and bottom by points. For a given body, however, different arrangements of the arbitrarily selected lamina give different results. The lamina method also has the disadvantage that the correct field of a body represented by laminas cannot be determined within or near a lamina. The facility to calculate anomalies near bodies would be useful in demagnetization calculations and in the interpretation of underground measurements or topographic effects.

The inaccuracy that results from use of the

Manuscript received by the Editor July 31, 1975; revised manuscript received January 5, 1976.

\* U.S. Geological Survey, Menlo Park, Calif. 94025.

© 1976 Society of Exploration Geophysicists. All rights reserved.

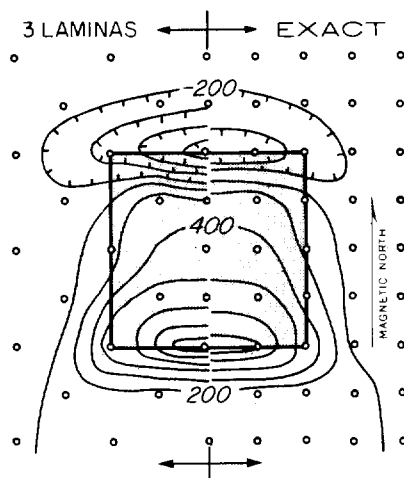


FIG. 1. Total magnetic field of three equally spaced laminas compared with exact field of rectangular prism. Contour interval is 200 gammas. Hachures on low side of contours. Each side of body is 4 units in length. Depth to top of prism is 0.15 unit and depth to bottom is 2.15 units.  $K = 0.005$  emu/cc.  $H = 0.4$  oersted.  $I_e = 60$  degrees. Laminas are located at the top, middle, and bottom of the prism. Open circles indicate location of field-points. Shaded pattern indicates location of prism. Note that the contour levels of the two models differ by about 200 gammas near the north and south edges of the prism.

lamina approximation, and the inability to calculate the field at the same level as the body, can be overcome by integrating the lamina formulas in the direction of depth to give an exact solution for a three-dimensional polygonal prism (Figure 1).

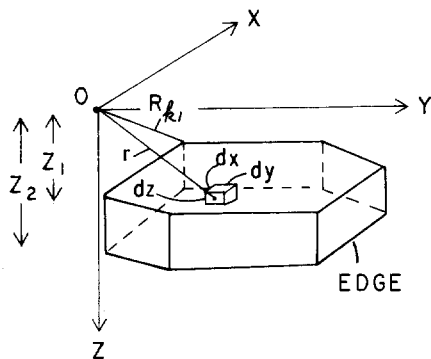
Thus, layers can be used instead of laminas. As shown in the following sections, the integrations are relatively elementary. But to my knowledge the integrations have not been reported, though several papers have been published recently on this subject (for example, Grant, 1972; Johnson and Litehiser, 1972; Goodacre, 1973; Whitehill, 1973). The gravity and magnetic values obtained by using formulas derived here have been checked by using models of rectangular prisms for which exact formulas previously have been published.

### SYMBOLS USED

The geometric relations of most of the symbols used in the following sections are shown in Figure 2. Exact definitions and supplementary notes-needed for a more complete derivation are given in the Appendix. Further details of the derivations are given by Plouff (1975a, b).

The gravity or magnetic effects of a polygonal prism are expressed in terms of the summation of the contributions from the individual edges of an  $n$ -sided prism. The summation progresses in a clockwise fashion around the prism as viewed from above. For the  $i$ th edge, paired terms occur that are functions of the coordinates at the endpoints of that edge. The subscript 1 refers to the first endpoint (or corner) of that edge found in the clockwise progression, and the subscript 2 refers to the latter of the two endpoints. The general subscript  $k$  refers to either of the endpoints. The depths  $z_j$  to the top or bottom face of the prism are expressed as absolute values, with the subscript 1 referring to the face closer to the field-

### BASIC ELEMENT - POLYGONAL PRISM



### PLAN VIEW OF ONE EDGE OF PRISM

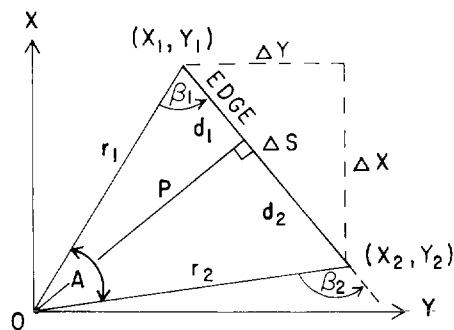


FIG. 2. Geometric elements involved in calculation of gravity and magnetic anomalies caused by a polygonal prism. The fieldpoint is located at the origin of the rectangular coordinate system.

point and the subscript 2 referring to the more distant face. Hence, the distance  $R_{kj} = \sqrt{r_k^2 + z_j^2}$ .

## GRAVITY

### Integration

The formula for the gravity effect corresponding to each edge of a horizontal polygonal lamina developed by Talwani and Ewing [1960, equation (5)] includes only terms that can be expressed in the form

$$A + \sin^{-1} \frac{C_k z}{\sqrt{P^2 + z^2}}, \quad (1)$$

where  $A$ ,  $C_k$ , and  $P$  are constants (see Appendix for conversion from the notation of Talwani and Ewing to that of this report). These terms can be expressed in the equivalent form

$$A = \tan^{-1} \frac{d_k z}{PR_k}.$$

A polygonal prism is formed by integrating a sequence of closely spaced, horizontal polygonal laminas with respect to the depth  $z$ . Integrating the lamina formula once by parts, and using Peirce's table (1929, p. 20, integral 129) after substituting a variable  $q^2$  for  $P^2 + z^2$ , gives terms of the form

$$Az = z \tan^{-1} \frac{d_k z}{PR_k} - \ln \left[ \frac{R_k + \frac{d_k}{P}}{\sqrt{P^2 + z^2}} \right] \quad (2)$$

for the gravity effect of each edge of a polygonal prism.

Substituting this integral for all terms in Talwani and Ewing's original equation, the vertical component of gravity caused by an  $n$ -sided polygonal prism with vertical sides is

$$\begin{aligned} g = \gamma \rho s_m \sum_{i=1}^n \left\{ s_p A[z_2 - z_1] \right. \\ + z_2 \left[ \tan^{-1} \frac{z_2 d_1}{PR_{12}} - \tan^{-1} \frac{z_2 d_2}{PR_{22}} \right] \\ - z_1 \left[ \tan^{-1} \frac{z_1 d_1}{PR_{11}} - \tan^{-1} \frac{z_1 d_2}{PR_{21}} \right] \\ \left. - P \ln \left[ \frac{R_{22} + d_2}{R_{12} + d_1} \frac{R_{21} + d_1}{R_{21} + d_2} \right] \right\}, \quad (3) \end{aligned}$$

where  $\gamma$  is the Universal Gravity Constant and  $\rho$  is the density of the prism. The symbol  $s_m = 1$  if the center of mass of the prism is below the field-

point and  $s_m = -1$  if the center of mass is above the fieldpoint. The symbol  $s_p = 1$  if  $P$  is positive, and  $s_p = -1$  if  $P$  is negative. For the special case of  $P = 0$ , the gravity value and volume subtended by the corresponding edge of the prism, as viewed from the fieldpoint, are zero. Computer time can be reduced by determining the sum of angles  $A$  outside the indicated summation. The sum is  $2\pi$  for the fieldpoints located over the interior of the polygon, zero for exterior points,  $\pi$  over an edge, and equal to the interior angle if the fieldpoint is located over the intersection of two edges of the polygon.

Kolbenheyer [1963, equation (11)] derived a formula similar to equation (3). But no provision was made for fieldpoints located over an edge or a corner of the polygonal prism. The arctangent terms of Kolbenheyer are of the form

$$\frac{P}{|P|} \tan^{-1} \frac{r^2 + dR}{|Pz|} = \tan^{-1} \frac{1}{Pz} + \tan^{-1} \frac{zd}{PR},$$

which are equivalent to the terms of equation (3), because paired terms of the form  $\tan^{-1} (1/Pz)$  at opposite ends of an edge are of equal magnitude and opposite sign.

### Comparison with rectangular prism

The formula for the gravity effect of a rectangular prism has been derived independently by the author for comparison with terrain correction approximation formulas (Plouff, 1966a). The formula is similar to that of Kellogg (1929, p. 57), and it provides a gravity value anywhere inside or outside the prism. The value of the vertical component of gravity is

$$\begin{aligned} g &= \gamma \rho \int_{a_1}^{a_2} \int_{b_1}^{b_2} \int_{z_1}^{z_2} \frac{z \, dz \, dy \, dx}{r^3} \\ &= \gamma \rho \sum_{i=1}^2 \sum_{j=1}^2 \sum_{k=1}^2 s \left[ z_k \tan^{-1} \frac{a_i b_j}{z_k R_{ijk}} \right. \\ &\quad \left. - a_i \ln(R_{ijk} + b_j) - b_j \ln(R_{ijk} + a_i) \right], \quad (4) \end{aligned}$$

where  $R_{ijk} = \sqrt{a_i^2 + b_j^2 + z_k^2}$  and  $s = s_i s_j s_k$  with  $s_1 = -1$  and  $s_2 = +1$ . Gravity values obtained by using a computer program that is based on equation (3), for any  $x$ - $y$  orientation of a rectangular prism, agree exactly with those obtained by using a computer program based on equation (4) (Plouff, 1975b, Table 6)

### Gravity prism example

A small network of gravity stations was established by the author in western Imperial Valley, Calif., in association with R. V. Sharp's study of Salton Trough tectonics. One of the principal features of the gravity map (Figure 3) is an elongated gravity high that seems well-suited for three-dimensional gravity interpretation. Three small hills of Cretaceous granodiorite that crop out along the crest of the gravity high indicate a ridge of basement rock buried at shallow depth under Quaternary deposits. Crystalline rock consisting of Cretaceous granitic rocks crop out at Superstition Mountain, and crystalline Cretaceous and older metamorphic rocks crop out at the Fish Creek Mountains (R. V. Sharp, oral communication, 1974). An arbitrary density of 2.00 gm/cc was used for the Bouguer reduction to sea level, as assumed by Kovach et al (1962), and terrain corrections were carried to 167 km using a density of 2.67 gm/cc.

A succession of models was tried in order to account for the positive gravity anomaly. The first model was a seven-sided polygonal prism that extended from 15 m (50 ft) above sea level to 457 m (1500 ft) below sea level, with sides approximately beneath the minus 31 m-gal contour level. The location of gravity gradients, especially along the northwest edge of the indicated model, suggests the presence of an uplifted fault block. The density contrast  $\rho$  and gravity datum  $g_a$  were determined to give the smallest deviation between the calculated and observed anomaly and to optimize the trial-and-error process. Equation (3) may be written  $g = \rho B$ . The least-squares process was used to determine the intercept  $g_a$  and the regression coefficient  $\rho$  in the equations

$$g_o = g_a + \rho B, \quad (5)$$

used for each station, where  $g_o$  is the observed anomaly and  $B$  is a function of the coordinates of the body under consideration. Station locations that were used for the determination of the subsurface model that seems to account for the observed gravity high are omitted from the residual gravity map (Figure 3).

A best density contrast of 0.52 gm/cc was determined for the indicated model. The average bulk density for samples collected from the two northern outcrops of granodiorite is 2.64 gm/cc which—with the determined density contrast—would give an average density of 2.12 gm/cc for the Qua-

ternary deposits between the surface and 762 m (2500 ft) below sea level. This average density for Quaternary deposits seems reasonable. A basement high remains to be fitted near the southeast corner of the residual gravity map. The gradients between the assumed model westward toward the Fish Creek Mountains and north-eastward toward Superstition Mountain could be removed by a trial-and-error process to build up the higher density rock from the base of the model to the surface where crystalline rock is exposed. The small, closed, residual gravity low (−39 mgal contour level) indicates that the Quaternary deposits probably are thicker in that vicinity before the basement rises northeastward to the surface at Superstition Mountain.

## MAGNETICS

### Solution of integration

The gravity effect of a polygonal prism has the simple form of equation (3) because only the vertical component of gravity is calculated, and density is a scalar quantity. Either the vertical or the total component of the magnetic anomaly, however, might be needed. Furthermore, the intensity of magnetization is a vector quantity. Therefore, the three orthogonal components of the magnetic anomaly,

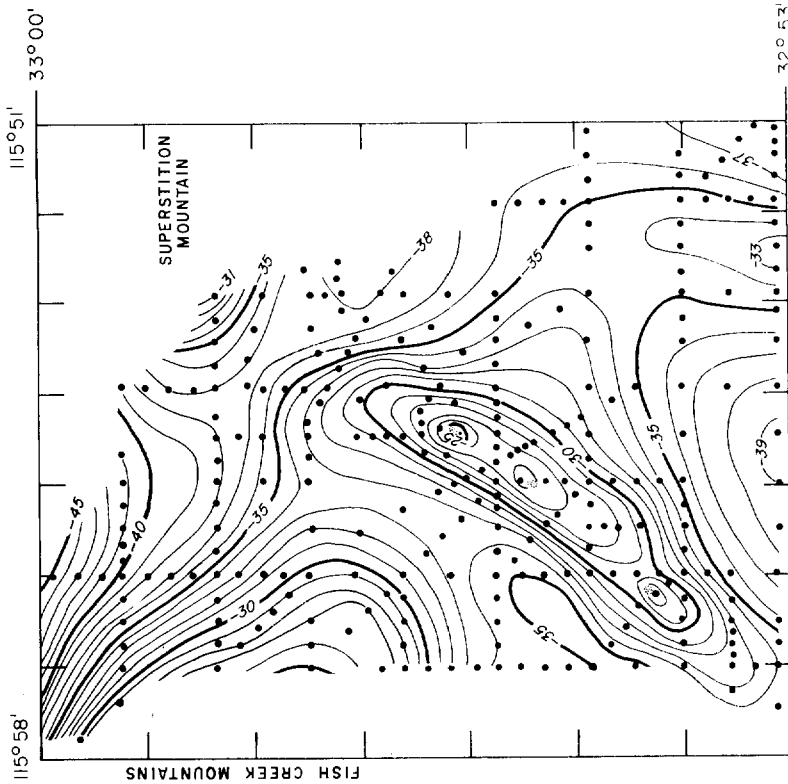
$$\begin{aligned} X &= J_x V_1 + J_y V_2 + J_z V_3, \\ Y &= J_x V_2 + J_y V_4 + J_z V_5, \\ Z &= J_x V_3 + J_y V_5 + J_z V_6 \end{aligned} \quad (6)$$

[Talwani, 1965, equation (2)], are calculated. The quantities  $X$ ,  $Y$ , and  $Z$  are the components of the magnetic field of an anomalous body in the direc-

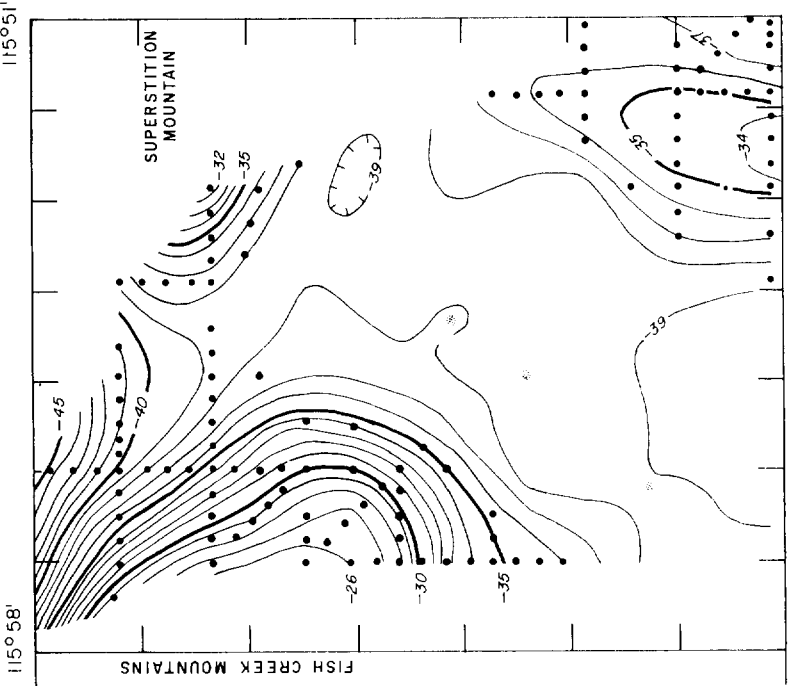


FIG. 3. Reduction of size of observed gravity anomaly by inferring the configuration of a buried mass that consists of eight polygonal prisms. Gravity contour interval is 1 mgal. Bouguer reduction density is 2.0 gm/cc. Topographic and body contours are expressed in feet relative to sea level. Topographic contour interval is 200 ft with labeled supplementary contours. Elevation of top of each body layer is labeled. The bottom of each layer coincides with the elevation of the top of the underlying layer and the elevation of the bottom of the lowest layer is 2500 ft below sea level. Locations of three small outcrops of Cretaceous granodiorite are indicated by dotted pattern. Large dots indicate locations of gravity stations.

TOPOGRAPHIC AND OBSERVED GRAVITY MAP



BODY CONTOUR AND RESIDUAL GRAVITY MAP



tion of the  $x$ -,  $y$ -, and  $z$ -axes, respectively (Figure 2). The quantities  $V_{1-6}$  are volume integrals defined by Talwani [1965, equation (3)]. The  $z$ -axis is always defined as parallel to the normal to the bases of the polygonal prism but is not necessarily vertical. Use of the  $x$ - and  $y$ -axes as horizontal and the  $z$ -axis as vertical, however, simplifies a display of the model with conventional elevation contours.

Excluding multiplicative constants, the expression for the magnetic effect of horizontal polygonal laminas includes terms of only three forms to be integrated in the direction of depth [Talwani, 1965, equation (4)]. These are (see Appendix for conversion from Talwani's notation to that of this report):

$$\frac{dz}{(z^2 + P^2)R_k}, \quad (7a) \quad \text{and}$$

$$\frac{z dz}{(z^2 + P^2)R_k}, \quad (7b)$$

and

$$\frac{z^2 dz}{(z^2 + P^2)R_k}. \quad (7c)$$

Term (7a) is integrated by using Peirce's (1929) integral 229a, noting that the hypotenuse  $r_k$  of a right triangle is never shorter than either of its legs  $P$  or  $d_k$ . Term (7b) is integrated by using Peirce's (1929) integral 230b. Term (7c) is integrated by substituting  $(z^2 + P^2) - P^2$  for  $z^2$  and using Peirce's (1929) integrals 126a and 229a for the two parts. The indefinite integrals of the terms (7a)–(7c) are

$$\frac{1}{Pd_k} \tan^{-1} \frac{zd_k}{PR_k}, \quad (8a)$$

$$\begin{aligned} \frac{1}{2d_k} \ln \left[ \frac{R_k - d_k}{R_k + d_k} \right] \\ = -\frac{1}{d_k} \ln \left[ \frac{R_k + d_k}{\sqrt{P^2 + z^2}} \right], \end{aligned} \quad (8b)$$

and

$$\ln(z + R_k) - \frac{P}{d_k} \tan^{-1} \frac{zd_k}{PR_k}, \quad (8c)$$

respectively.

Talwani [1965, equation (4)] has solved for surface integrals  $S$  to determine the above volume integrals  $V$  by using the lamina approximation  $V \approx S \Delta z$ . The exact value for a prism, however, is

$V = \int S dz$ . The integration is accomplished, as indicated above, by obtaining terms (8a)–(8c) from terms of the form (7a)–(7c). Therefore,

$$V_1 = \sum_{i=1}^n (SCF - C^2W),$$

$$V_2 = \sum_{i=1}^n (SCW + C^2F),$$

$$V_3 = \sum_{i=1}^n CQ,$$

$$V_4 = -\sum_{i=1}^n (SCF + S^2W),$$

$$V_5 = -\sum_{i=1}^n SQ,$$

$$V_6 = \sum_{i=1}^n W, \quad (9)$$

for a polygonal prism, where

$$F = \ln \left[ \frac{R_{22} + z_2}{R_{12} + z_2} \frac{R_{11} + z_1}{R_{21} + z_1} \right],$$

$$Q = \ln \left[ \frac{R_{22} + d_2}{R_{12} + d_1} \frac{R_{11} + d_1}{R_{21} + d_2} \right],$$

and

$$\begin{aligned} W = \tan^{-1} \frac{z_2 d_2}{PR_{22}} - \tan^{-1} \frac{z_2 d_1}{PR_{12}} \\ - \tan^{-1} \frac{z_1 d_2}{PR_{21}} + \tan^{-1} \frac{z_1 d_1}{PR_{11}}. \end{aligned}$$

If the fieldpoint is located on any edge of the prism, a singularity is produced by the logarithm terms of equation (9). An example of the effect of approaching the edge of a magnetic body is indicated in Table 1. A similar logarithmic term appears in the expression for the magnetic anomaly at a corner of two-dimensional bodies (Reford and Summer, 1964, p. 505). This location is impossible in practice because the magnetic sensor is a finite size. My computer program (Plouff, 1975a) arbitrarily moves the location of a fieldpoint upward a height of 0.002 times the thickness of the thinnest layer of the model in order to bypass accidental coincidence of a fieldpoint with an edge of the model when polygonalized topographic contours are constructed.

### Components of the magnetic field

The magnetic anomaly for a polygonal prism is calculated by substituting values from equation (9) into equations (6). The  $z$ -axis need not be vertical in the  $x$ - $y$ - $z$  coordinate system if the definition of the  $J$ -components are consistent with the choice of axes, but display of the model is simplified, and direct reference to conventional definitions of magnetic inclination and declination can be used with the choice of the  $z$ -axis as the depth coordinate. Because the time of calculation of the summations indicated in equations (9) is considerably longer than the simple multiplications indicated in equations (6), proportionally little execution time is expended by calculating the values of  $V$  once for several combinations of  $J$ -components.

The change  $T$  in the total magnetic field at an observation point owing to the presence of an anomalous body can be determined from the equation

$$T = \sqrt{(lH + X)^2 + (mH + Y)^2 + (nH + Z)^2} - H, \quad (10)$$

where  $l$ ,  $m$ ,  $n$  are the direction cosines of the earth's field (see Appendix),  $H$  is magnitude of the earth's field, and  $X$ ,  $Y$ , and  $Z$  are the magnetic

components of the anomalous body, as calculated in equation (6). If the anomaly  $T$  caused by a magnetic body is small compared to the main field  $H$ , then  $T$  can be approximately measured by projecting the components of the anomalous field in the direction of the earth's field. Therefore,

$$T \approx lX + mY + nZ. \quad (11)$$

Substituting values of  $X$ ,  $Y$ , and  $Z$  from equation (6) into equation (11),

$$\begin{aligned} T &= J_x(lV_1 + mV_2 + nV_3) \\ &\quad + J_y(lV_4 + mV_5 + nV_6) \\ &\quad + J_z(lV_7 + mV_8 + nV_9) \\ &= J_xB_1 + J_yB_2 + J_zB_3, \end{aligned} \quad (12)$$

where  $B_1$ ,  $B_2$ , and  $B_3$  are functions of body coordinates using  $V$  calculated in equation (9).

Equation (12) can be used to solve for the  $J$ -

**Table 1.** Change in value of  $V_3$  as edge of rectangular prism is approached. [The prism is 2 by 6 units in horizontal dimensions and 3.125 units in depth. The  $x$ -axis (increasing values to north) is parallel to the long side of the prism, and the origin of the coordinate axes is at the center of the prism. Column headings indicate fieldpoint height relative to the top of the prism. Values are symmetric with respect to the plane  $y = 0$ . Values are symmetric but algebraic signs are reversed with respect to the plane  $x = 0$ .]

| $x$ | $y$ | 0.1 | 0.001 | 0.00001 | zero     |
|-----|-----|-----|-------|---------|----------|
| -4  | 0.0 | 1.1 | 1.1   | 1.1     | 1.1      |
| -4  | 0.5 | 1.1 | 1.1   | 1.1     | 1.1      |
| -4  | 1.0 | 0.8 | 0.8   | 0.8     | 0.8      |
| -4  | 1.5 | 0.6 | 0.6   | 0.6     | 0.6      |
| -3  | 0.0 | 5.3 | 14.5  | 23.7    | $\infty$ |
| -3  | 0.5 | 5.1 | 14.3  | 23.5    | $\infty$ |
| -3  | 1.0 | 3.1 | 7.7   | 12.3    | $\infty$ |
| -3  | 1.5 | 1.0 | 1.0   | 1.0     | 1.0      |
| -2  | 0.0 | 1.1 | 1.1   | 1.1     | 1.1      |
| -2  | 0.5 | 1.0 | 1.0   | 1.0     | 1.0      |
| -2  | 1.0 | 0.8 | 0.8   | 0.8     | 0.8      |
| -2  | 1.5 | 0.6 | 0.6   | 0.6     | 0.6      |
| -1  | 0.0 | 0.3 | 0.3   | 0.3     | 0.3      |
| -1  | 0.5 | 0.3 | 0.3   | 0.3     | 0.3      |
| -1  | 1.0 | 0.3 | 0.3   | 0.3     | 0.3      |
| -1  | 1.5 | 0.2 | 0.2   | 0.2     | 0.2      |
| 0   | 0.5 | 0.0 | 0.0   | 0.0     | 0.0      |
| 0   | 1.0 | 0.0 | 0.0   | 0.0     | 0.0      |

components of the intensity of magnetization by a least-squares comparison of the observed magnetic anomalies  $T_o$ , with the calculated magnetic anomalies  $T$  in the equation

$$\begin{aligned} T_o &= T_d + T \\ &= T_d + J_xB_1 + J_yB_2 + J_zB_3, \end{aligned} \quad (13)$$

for four or more fieldpoints, where  $T_d$  is value determined for a nominal magnetic datum shift. The values for  $T_d$ ,  $J_x$ ,  $J_y$ , and  $J_z$  can be determined by multiple regression formulas such as those described by Arkin and Colton (1956, page 94). Ignoring the effect of demagnetization, the components of the total magnetization vector needed in equation (13) are

$$J_x = KHI + J_rL,$$

$$J_y = KHM + J_rM,$$

and

$$J_z = KHN + J_rN, \quad (14)$$

where  $K$  is the magnetic volume susceptibility,  $J_r$  is the intensity of remanent magnetization, and  $L$ ,  $M$ , and  $N$  are the direction cosines of the remanent magnetization vector. If the magnetic sus-

ceptibility of the anomalous body is small compared to the remanent magnetization, the substitution  $K=0$  can be made in equation (14). Then, equation (13) becomes

$$T_o = T_d + J_r L B_1 + J_r M B_2 + J_r N B_3, \quad (15)$$

and the magnitude  $J_r$  of the remanent (or total) magnetization vector with its declination  $D_r$  and inclination  $I_r$ , as defined in the Appendix, can be easily determined.

If the remanent magnetization of an anomalous body is small compared to its magnetic susceptibility, the substitution  $J_r = 0$  can be made in equation (14). Substituting for the  $J$ -components in equation (13),

$$\begin{aligned} T_o &= T_d + KH(1B_1 + mB_2 + nB_3) \\ &= T_d + KB, \end{aligned} \quad (16)$$

where  $B$  is a function of the body coordinates. Equation (16), as applied to two or more field points, can be solved for the regression coefficient  $K$  and apparent magnetic susceptibility that depends on the observed magnetic anomalies  $T_o$  and the calculated magnetic anomalies  $T = KB$ .

#### Comparison with rectangular prism

Magnetic values obtained by using a computer program, based on equations (6) and (9) for the special case of a rectangular prism, exactly agree with those obtained by using a computer program based on the magnetic values for a rectangular prism (Plouff, 1975a, p. 98). The comparison was made by using my equations that are similar to those of Bhattacharyya (1964), Sharma (1966), and Goodacre (1973) for the magnetic effect of rectangular prism.

For a rectangular prism,

$$V_1 = \int_{z_1}^{z_2} \int_{b_1}^{b_2} \int_{a_1}^{a_2} \left( \frac{3x^2}{R^5} - \frac{1}{R^3} \right) dx dy dz,$$

is solved by using Peirce's (1929) integrals 174, 138, and 229, respectively. The triplet  $(a_i, b_j, z_k)$  denotes the location of a corner relative to a field-point. Next,

$$V_2 = \int_{z_1}^{z_2} \int_{b_1}^{b_2} \int_{a_1}^{a_2} \frac{3xy}{R^5} dx dy dz,$$

is solved by using Peirce's (1929) integrals 171, 140, and 126a. Values for  $V_3$ – $V_6$  are obtained by direct integration or by cyclic permutation of  $x$ – $y$ – $z$  and  $a_i$ – $b_j$ – $z_k$  in the values for  $V_1$  and  $V_2$ .

Hence,

$$V_1 = - \sum_{i=1}^2 \sum_{j=1}^2 \sum_{k=1}^2 s \tan^{-1} \frac{b_j z_k}{a_i R_{ijk}},$$

$$V_2 = \sum_{i=1}^2 \sum_{j=1}^2 \sum_{k=1}^2 s \ln (R_{ijk} + z_k),$$

$$V_3 = \sum_{i=1}^2 \sum_{j=1}^2 \sum_{k=1}^2 s \ln (R_{ijk} + b_j),$$

$$V_4 = - \sum_{i=1}^2 \sum_{j=1}^2 \sum_{k=1}^2 s \tan^{-1} \frac{a_i z_k}{b_j R_{ijk}},$$

$$V_5 = \sum_{i=1}^2 \sum_{j=1}^2 \sum_{k=1}^2 s \ln (R_{ijk} + a_i),$$

and

$$V_6 = - \sum_{i=1}^2 \sum_{j=1}^2 \sum_{k=1}^2 s \tan^{-1} \frac{a_i b_j}{z_k R_{ijk}}, \quad (17)$$

where  $R_{ijk} = \sqrt{a_i^2 + b_j^2 + z_k^2}$  and  $s = s_i s_j s_k$  with  $s_1 = -1$  and  $s_2 = +1$ .

#### Magnetic terrain correction examples

Magnetic models can be obtained by using a trial-and-error process similar to that used in the example for a gravity model. If magnetic rocks crop out, polygonal prism formulas can be used to determine a magnetic terrain correction. Richards et al (1967) discussed a number of useful examples in which magnetization parameters were obtained

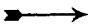
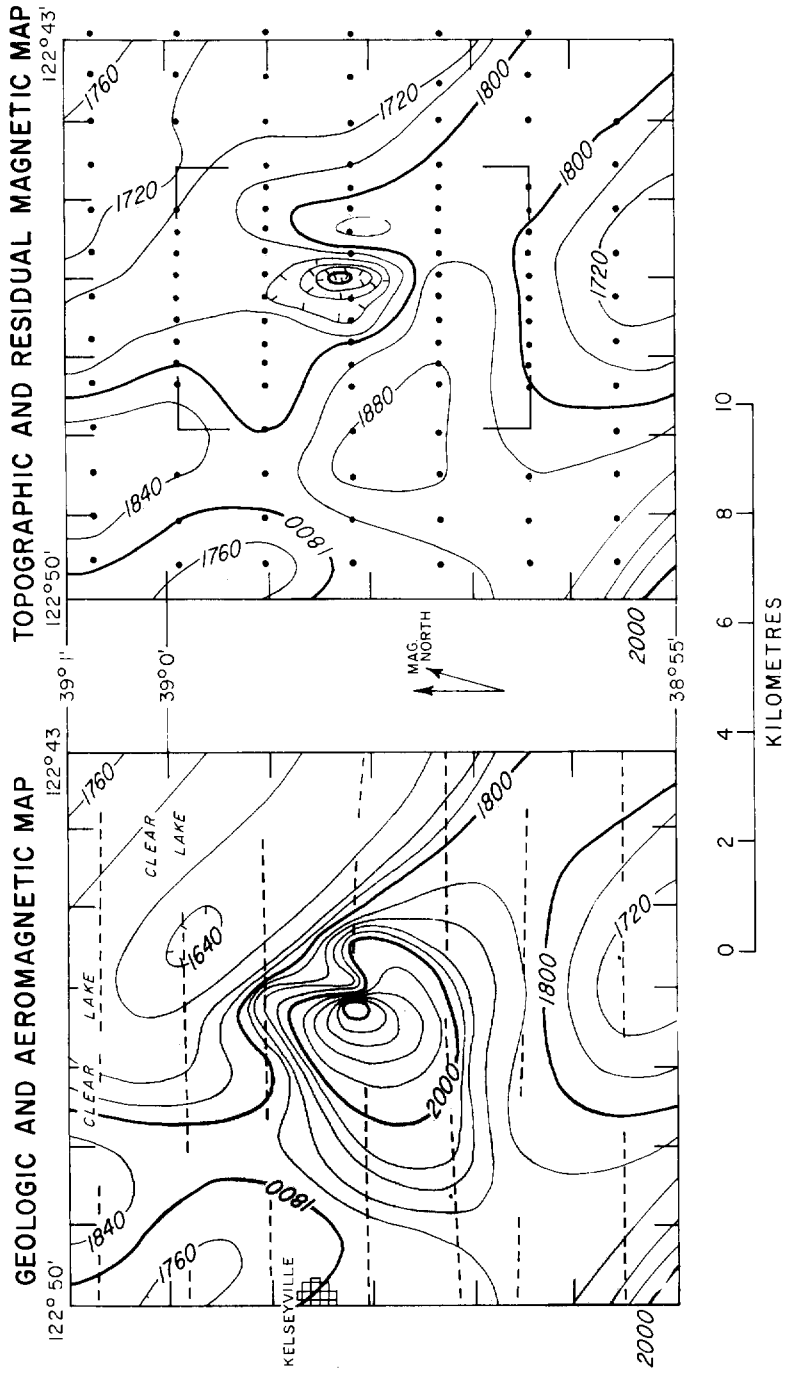


FIG. 4. Reduction in size of observed aeromagnetic anomaly by removing the effect of topography with an assumed constant magnetic susceptibility. Aeromagnetic map adapted from U.S.G.S. (1973). Contours show total intensity magnetic field of the earth in gammas relative to an arbitrary datum. Contour interval is 40 gammas. Dashed lines indicate flight path. Survey flown at 1372 m (4500 ft) barometric elevation. Hachures are on low side of magnetic contours. Shaded pattern on geologic map indicates location of unit of Quaternary dacite and andesite (adapted from Brice, 1953; McNitt, 1968a, b). Dotted line on geologic map indicates location of edge of Clear Lake, Calif. Polygonalized topographic contours are generalized from standard 15-minute maps of the U.S.G.S. Topographic contours are labeled in units of hundreds of feet above sea level; interval is 400 ft with an additional contour at 3800 ft above sea level. Dots on residual magnetic map indicate position where magnetic field is calculated. L-shaped symbols indicate corners of area in which calculated values were used for a least-squares determination of the best magnetic susceptibility contrast.





by comparing observed magnetic anomalies with rectangularly gridded topography. The use of polygonal prisms by polygonalization (replacing curved lines with a finite number of straight line segments) of topographic contours, however, is an easier procedure to apply and provides a more realistic representation of topography.

The magnetic effect of a prominent magnetic high over Mt. Konocti, near Clear Lake, Calif. (Figure 4), was largely removed by applying a magnetic terrain correction. The apparent magnetic susceptibility [equation (16)] for the topographic model was computed for two reasons, although remanent magnetization is present in sample measurements. First, the volcanic rocks are relatively young and probably are not rotated from their original position (C. B. Hearn, 1974, oral communication); therefore remanent magnetization, if present, is probably aligned nearly parallel to the present earth's field. Second, the contributions of a prominent magnetic low, superimposed on the east edge of the high and on the east edge of the unknown deeper rocks beneath the level of the polygonalized topography, might interfere with obtaining the true magnetization direction when the more general equation (13) is applied.

A preliminary calculation was made for a topographic model with a base level at 488 m (1600 ft) above sea level, which resulted in a best-susceptibility of 0.0035 emu/cc. Next, a model with a base level of 366 m (1200 ft) above sea level was tested, which resulted in a best-susceptibility of 0.0033 emu/cc. The latter model was used to produce the residual map in Figure 5 because the coefficient of correlation between the observed and calculated anomalies improved from 88 to 92 percent, where 100 percent would be perfect agreement. This useful statistical test, equivalent to the goodness-of-fit test of Richards et al (1967), provided an objective criterion for extending this volcanic unit downward into a calderalike form. A prominent residual magnetic low, however, remained to be explained. Nearby occurrences of olivine basalt float of low magnetization (C. B. Hearn, 1974, oral communication) suggest the existence of a larger concealed mass of similar rock with low magnetization above 1067 m (3500 ft) elevation east of the crest of Mt. Konocti. Truckborne magnetometer traverses at lower elevations to the south and west indicated large variations of magnetization within this Quaternary volcanic unit by recording changes up to 2000 gammas in 0.5 km

distance. Residual magnetic highs that nearly encircle the magnetic low indicate that, except at the location of magnetic low, the total magnetization (expressed in terms of magnetic susceptibility) should be higher than the computed value.

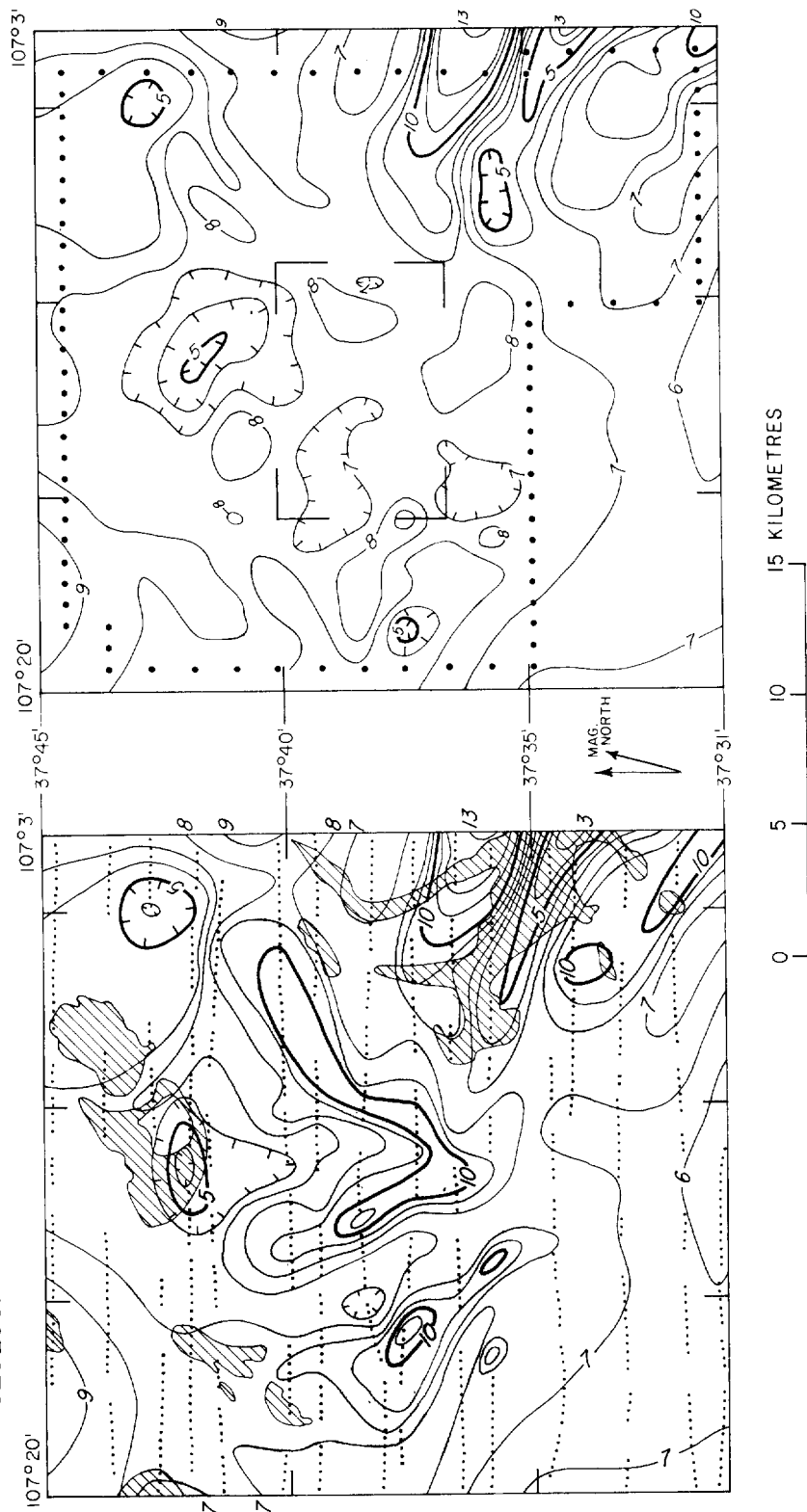
A substantial reduction in the size of a prominent V-shaped magnetic anomaly (Figure 5), located near the southwest edge of the San Juan Mountains, Colo., was similarly achieved by applying a magnetic terrain correction. The topography that was polygonalized corresponds to the area of outcrop of the Huerto Formation, a Tertiary volcanic unit that consists of dark andesitic flows and breccias (Steven et al, 1969). Using equation (15), a "best" intensity of total magnetization of 0.0040 emu/cc was determined for a test area and applied to a larger area in order to derive a residual map (Figure 5). Ignoring the effect of magnetic susceptibility, the best declination is N7W, the best inclination is 42 degrees downward, and the coefficient of multiple correlation, relating the calculated to the observed anomalies in the test area, is 89 percent. Modeling the topography was complicated by the northward wedging-out of the Huerto Formation, the occurrence of faults boundaries for the southeast outcrops, and the need to exclude overlying formations and estimate the position of the concealed lower contact of the Huerto Formation. Despite these



FIG. 5. Reduction in size of observed aeromagnetic anomaly by removing the effect of topography with an assumed constant magnetization. Aeromagnetic map adapted from Popenoe and Steven (1969). Contours show total intensity magnetic field of the earth in units of hundreds of gammas relative to an arbitrary datum. Contour interval is 100 gammas. Dotted lines on aeromagnetic map indicate flight path. Survey flown at 4267 m (14,000 ft) barometric elevation. Hachures on low side of magnetic contours. Topographic contours are labeled in units of thousands of feet above sea level; interval is 500 ft. Shaded pattern indicates location of the Huerto Formation and striped pattern indicates location of Carpenter Ridge Tuff on geologic map (Steven et al, 1969). Polygonalized topographic contours that depict a model of the Huerto Formation are generalized from Steven et al (1969). Dashed contours indicate estimated position of concealed edge of Huerto Formation. Dots indicate boundary of uniformly spaced gridwork of positions where magnetic field is calculated. L-shaped symbols indicate corners of area in which calculated values were used for a least-squares determination of the best magnetic susceptibility contrast.

GEOLOGIC AND AEROMAGNETIC MAP

TOPOGRAPHIC AND RESIDUAL MAGNETIC MAP



problems, and the coarseness of the selected contour intervals for modeling topography, the relatively small residual anomaly indicates success of this analysis.

The residual magnetic map (Figure 5) includes some apparent correlations with topography that indicate large-scale variations of magnetization within the Huerto Formation. For example, the elongated magnetic high enclosed by the 800- and 900-gamma contours and the nearly circular low enclosed by the 500- and 600-gamma contours (located to the west of the test area) indicate higher and lower rock magnetizations, respectively, compared to the nominal value determined in the least-squares process. The residual closed low located to the north of the test area no longer extends downward to the 400-gamma level because the dipole-low effect to the north of the model has been removed. This residual low and the low to the northeast is mostly related to the effect of the reversely magnetized Carpenter Ridge Tuff (Popenoe and Steven, 1969), a crystal-poor rhyolite welded tuff of Tertiary age (Olson et al, 1968; Steven et al, 1969). The magnetic ridge between the two lows (Figure 5) reflects the absence of rock in the topographic low between the two outcrops of Carpenter Ridge Tuff. The narrow magnetic low that extends more than 16 km southeastward from the closed residual low at the 500-gamma level, located near the southeast corner of the area, indicates the strongly reversed magnetization of the Carpenter Ridge Tuff.

### DISCUSSION

Existing computer programs, including interactive graphics programs based on the gravity or the magnetic effect of rectangular prisms, can be replaced by the more general polygonal prism programs with the exception of programs using rectangularly gridded models or automated inversion programs, such as that suggested by Whitehill (1973). Inversion programs, however, can be coordinated with polygonal prism programs to the advantage of both. For example, the 3-D iterative gravity program of Cordell and Henderson (1969) can be used to minimize the trial-and-error aspect of the polygonal prism program. A more realistic-appearing contoured representation of the model generated by the iterative program can then be used as initial input to the polygonal prism program, after which additional refinements can be made. The existence of duplicated terms, that are summed in polygonal prism

equations (3) and (9) and rectangular prism equations (4) and (17), would optimize a coordination between gravity and magnetic programs.

Except for the need to ignore the effect of demagnetization and avoid locations on the edges of magnetic models, equations (3) or (9) can be used to determine the respective gravity or magnetic anomalies anywhere outside or inside the polygonal prism. Therefore, these equations can be applied to interpret measurements in conditions such as drape-flying, tunnels, and boreholes. Examples were given in an earlier section where residual aeromagnetic maps that result from determining magnetic terrain corrections can be used to aid geologic mapping. Topography also can be polygonalized to provide magnetic terrain corrections for ground surveys. Modeling topography in the form of layers of polygonal prisms is particularly adapted for magnetic calculations because of the sensitivity of using the geometry of the upper and lower faces of the model (except near the equator) to express the polarized magnetic effect of the model.

Polarization, however, is not involved in the gravity effect of an anomalous body. Therefore the building blocks used to construct a model for gravity terrain corrections can take other forms. Gridded models that incorporate rectangular prisms were suggested by Bott (1959) and Kane (1962). These authors substituted the effect of a part of an annular ring (cylindrical compartment) as an approximation for a rectangular prism to avoid the expense of calculating equation (4). Bott (1959) also suggested the further approximation of concentrating the mass of the prism along a vertical line element located at its center. This approximation was applied by Plouff (1966a, 1966b) to rectangularly gridded compartments with geographic boundaries. The line-element approximation results in smaller but more accurate gravity values near the fieldpoint, as compared to rectangular or polygonal prisms. The line-element gravity values are more accurate because the ground surface near the fieldpoint tends to slope on the average through the location of the fieldpoint, rather than to be horizontal with sharp vertical boundaries at arbitrary locations, as assumed for the prism models.

Gridded models of terrain, unlike polygonalized models, permit correction for the effect of the earth's curvature and also have the advantage of using cost-saving approximations without loss of accuracy. This is done in gridded models

by using the apparent elevations of the top and bottom of the rectangular prism or line element as viewed along the horizon of the fieldpoint. Adding finer detail or expanded information to a polygonalized model is cumbersome, compared to universally gridded models (Plouff, 1966), where various levels of rectangular compartment sizes can be added to the model in blocks—"maps". Only one map needs to reside in the computer memory at a time in this system, whereas topographic information for an entire region must be stored in polygonal systems. At locations far from the fieldpoint, a coarse grid can be used with little loss in accuracy, whereas the polygonalized model would require time-consuming calculation of unnecessarily fine elements of topography.

Despite the disadvantages of polygonalization methods compared to grid methods as applied to gravity terrain corrections, magnetic terrain corrections seem well adapted to the polygonal prism concept. Computer costs related to preparing the examples of the present report tended to be minimized at the expense of human costs, by using hand methods of polygonalization which subjectively produce fewer polygon edges than would digitizing-machine methods. The effectiveness of three-dimensional model programs is greatly enhanced by a contour display of the results. Excluding plotter costs and the use of hand polygonalization, the central processor time needed to execute the contour program used to obtain the results in this paper was approximately the same as the computer time needed for calculating the anomalies. The execution time for calculating the gravity or magnetic effects of polygonal prisms approaches 1.6 msec/fieldpoint/edge on an IBM 370 computer. By comparing the basic formulas, it is estimated that the computer time used for calculating the gravity or magnetic effect of a prism is less than the computer time needed to calculate the effect of two polygonal laminas that might replace the prism. The representation of a prism by only two laminas, however, would result in dubious values (Figure 1), negating any possible savings in cost when using laminas.

#### ACKNOWLEDGMENTS

Andrew Griscom suggested the need for improvement of existing lamina and rectangular prism programs. William F. Hanna suggested methods of solution for three integrations needed for magnetic bodies and gave continued support

during program development. Robert V. Sharp suggested and supported gravity measurements associated with his studies of Salton Trough tectonics. Manik Talwani supplied the Lamont-Doherty Geological Observatory computer programs that formed the basis for the present research.

#### REFERENCES

- Arkin, H., and Colton, R. R., 1956, *Statistical methods*: 4th ed., New York, Barnes and Noble, 273 p.
- Bhattacharyya, B. K., 1964, Magnetic anomalies due to prism-shaped bodies with arbitrary polarization: *Geophysics*, v. 29, p. 517-531.
- Bott, M. P. H., 1959, The use of electronic digital computers for the evaluation of gravimetric terrain corrections: *Geophys. Prosp.*, v. 7, p. 45-54.
- , 1963, Two methods applicable to computers for evaluating magnetic anomalies due to finite three-dimensional bodies: *Geophys. Prosp.*, v. 11, p. 292-299.
- Brice, J. C., 1953, *Geology of the Lower Lake quadrangle, California*: Calif. Div. of Mines Bull. 166, 72 p.
- Cordell, L., and Henderson, R. G., 1968, Iterative three-dimensional solution of gravity anomaly data using a digital computer: *Geophysics*, v. 33, no. 4, p. 596-601.
- Goodacre, A. K., 1973, Some comments on the calculation of the gravitational and magnetic attraction of a homogeneous rectangular prism: *Geophys. Prosp.*, v. 21, p. 66-69.
- Grant, F. S., 1972, Review of data processing and interpretation methods in gravity and magnetics, 1964-71: *Geophysics*, v. 37, p. 647-661.
- Johnson, L. R., and Litehiser, J. J., 1972, A method for computing the gravitational attraction of three-dimensional bodies in a spherical or ellipsoidal earth: *J. Geophys. Res.*, v. 77, p. 6999-7009.
- Kane, M. F., 1962, A comprehensive system of terrain corrections using a digital computer: *Geophysics*, v. 27, p. 455-462.
- Kellogg, O. D., 1929, *Foundations of potential theory*: Berlin, Julius Springer, 384 p. [reprinted in 1953 by Dover Publications, New York].
- Kolbenheyer, T., 1963, Beitrag zur Theorie der Schwerkraftwirkungen homogener prismatischer Körper: *Studia Geoph. et Geod., Československá Akad. Věd.*, p. 233-239.
- Kovach, R. L., Allen, C. R., and Press, Frank, 1962, Geophysical investigations in the Colorado delta region: *J. Geophys. Res.*, v. 67, p. 2845-2871.
- McNitt, J. R., 1968a, *Geology of the Kelseyville quadrangle, Sonoma, Lake, and Mendocino Counties, California*: Calif. Div. of Mines and Geology Map Sheet 9.
- , 1968b, *Geology of the Lakeport quadrangle, Lake County, California*: Calif. Div. of Mines and Geology Map Sheet 10.
- Olson, J. C., Hedlund, D. C., and Hansen, W. R., 1968, Tertiary volcanic stratigraphy in the Powderhorn-Black Canyon region, Gunnison and Montrose Counties, Colorado: *U.S. G. S. Bull.* 1251-C, p. C1-C29.
- Peirce, B. O., 1929, *A short table of integrals*: Boston, Ginn, 156 p.
- Plouff, Donald, 1966, Digital terrain corrections based on geographic coordinates: Paper presented at the

- 36th Annual International SEG Meeting, November 10 in Houston. Abstract, Geophysics, v. 31, p. 1208.
- 1975a, Derivation of formulas and FORTRAN programs to compute magnetic anomalies of prisms: Natl. Tech. Inf. Service No. PB-243-525, U.S. Dept. Commerce, Springfield, Va., 112 p.
- 1975b, Derivation formulas and FORTRAN programs to compute gravity anomalies of prisms: Natl. Tech. Inf. Service No. PB-243-526, U.S. Dept. Commerce, Springfield, Va., 90 p.
- Popenoe, P., and Steven, T. A., 1969, Interpretation of the aeromagnetic pattern of the San Juan Primitive area, Colorado: U.S.G.S. open-file rep., 7 p.
- Reford, M. S., and Sumner, John, 1964, Review article-aeromagnetics: Geophysics, v. 29, p. 482-516.
- Richards, M. L., Vacquier, V., and Van Voorhis, G. D., 1967, Calculation of the magnetization of uplifts from combining topographic and magnetic surveys: Geophysics, v. 32, p. 678-707.
- Sharma, P. V., 1966, Rapid computation of magnetic anomalies and demagnetization effects caused by bodies of arbitrary shape: Pure and Appl. Geophys., v. 64, p. 89-109.
- Steven, T. A., Schmitt, L. J., Jr., Sheridan, M. J., and Williams, F. E., 1969, Mineral resources of the San Juan Primitive area, Colorado: U.S.G.S. Bull. 1261-F, 187 p.
- Talwani, M., 1965, Computation with help of a digital computer of magnetic anomalies caused by bodies of arbitrary shape: Geophysics, v. 30, p. 797-817.
- Talwani, M., and Ewing, M., 1960, Rapid computation of gravitational attraction of three-dimensional bodies of arbitrary shape: Geophysics, v. 25, p. 203-225.
- U.S. Geological Survey, 1973, Aeromagnetic map of Clear Lake area, Lake, Sonoma, Napa, and Mendocino Counties, California: U.S.G.S. open-file map.
- Whitehill, D. E., 1973, Automated interpretation of magnetic anomalies using the vertical prism model: Geophysics, v. 38, p. 1070-1087.

## APPENDIX

### DEFINITIONS

Symbols in Talwani's notation are indicated in parentheses. Where a symbol in parentheses occurs only on the left side of an equal sign, the symbol does not appear in the main sections of the present paper but was used in the derivation. The subscript  $k$  refers to either the vertex  $i$  or  $i+1$  of the  $i$ th side of the polygon. The subscript  $e$  refers to the earth's magnetic field, and the subscript  $r$  refers to the remanent magnetic field.  $D$  is the cylindrical angle of declination measured positive clockwise from the direction of the positive  $x$ -axis.  $I$  is the spherical angle of inclination measured positive downward.  $H$  is the magnetic field strength of the earth's field.  $J_r$  is the intensity of remanent magnetization. If  $H$  arbitrarily is set equal to zero, then  $J_r$ ,  $L$ ,  $MN$ ,  $D_r$ , and  $I_r$  refer to the total magnetization of the induced and remanent fields.  $K$  is magnetic volume susceptibility. The product  $KH$  is the intensity of induced magnetization.

### LIST OF DEFINITIONS

$$\begin{aligned}
 A &= \cos^{-1} [(x_1x_2 + y_1y_2)/(r_1r_2)] = (\Delta\psi) \\
 (c_{11}) &= P/S \\
 C &= \Delta y/\Delta s \\
 C_k &= -(x_k \Delta x + y_k \Delta y)/(r_k \Delta s) = \cos \beta_k \\
 d_k &= x_k S + y_k C = -r_k C_k \\
 (g_i) &= P/C \\
 l &= \cos I_e \cos D_e \\
 L &= \cos I_r \cos D_r \\
 m &= \cos I_e \sin D_e \\
 M &= \cos I_r \sin D_r \\
 n &= \sin I_e \\
 N &= \sin I_r \\
 P &= (x_1y_2 - x_2y_1)/\Delta s = x_k C - y_k S = (p_i) \\
 r^2 &= x^2 + y^2 + z^2 \\
 r_k^2 &= x_k^2 + y_k^2 = d_k^2 + P^2 \\
 R_k^2 &= r_k^2 + z^2 \\
 R_{k,j}^2 &= r_k^2 + z_j^2 \\
 S &= \Delta x/\Delta s \\
 \Delta s &= \sqrt{(\Delta x)^2 + (\Delta y)^2} = |d_1 - d_2| \\
 \Delta x &= x_2 - x_1 \\
 \Delta y &= y_2 - y_1 \\
 \beta_k &= (\theta_1 \text{ or } \phi_i \text{ for gravity}) = (\beta_i \text{ or } \gamma_i \text{ for magnetics})
 \end{aligned}$$

### SUPPLEMENTARY NOTES

Repeated use of the relation,

$$\tan^{-1} \frac{a+b}{1-ab} = \tan^{-1} a + \tan^{-1} b,$$

is made in equations (3), (4), (9), and (17) to decrease computer times. Two forms of the logarithm terms

$$\ln [(R+d)/\sqrt{P^2+z^2}] =$$

$$0.5 \ln [(R+d)/(R-d)],$$

appear when alternate methods of integration are used. The form on the left is used throughout the paper because the denominator of that term is not a function of the horizontal coordinates and cancels when paired terms are combined. The form on the right would require two tests instead of one for  $R \approx |d|$ .

If the perpendicular distance  $P$  from the field-point to a vertical side of the polygonal prism is zero, then the volume contribution of that side is zero and the gravity contribution [equation (3)] is zero. For magnetics, if  $P = 0$ , then  $W = 0$  and  $V_g = 0$  [equation (9)]. The values of the other volume integrals, however, are not zero, because Talwani's original definitions of integration direc-

tions have been retained. Integrals  $V_1$ ,  $V_2$ , and  $V_3$  are taken over the volume between the given side of the prism and the plane  $x = 0$ , while integrals  $V_4$  and  $V_5$  represent the volume between that side and the plane  $y = 0$ .

Also referring to equation (9), if  $P = z = 0$ ,  $d_1 < 0$ , and  $d_2 < 0$ , then  $(R_{11} + d_1)/(R_{21} + d_2) = d_2/d_1$ . If  $(P^2 + z_1^2) \ll d_k^2$  and  $d_k < 0$ , then the substitution,  $(R_{k1} + d_k) \simeq -(P^2 + z_1^2)/(2d_k)$ , is

needed to retain significant figures and to prevent calculating the logarithm of a digitally computed zero. Use of the relation  $V_4 = -(V_1 + V_5)$  permits some savings in computer time and array storage reduction. If the prism is located above the field-point, the algebraic sign of answers obtained by using equation (9) should be reversed, in order to retain absolute values for depths and a clockwise progression of vertices.